Supporting Information for

Enhanced In-source Fragmentation Annotation Enables Novel Data Independent Acquisition and Autonomous METLIN Molecular Identification

Jingchuan Xue[1,#], Xavier Domingo-Almenara[2,#], Carlos Guijas[1], Amelia Palermo[1], Markus M Rinschen[1], John Isbell[3], H. Paul Benton[1], and Gary Siuzdak[1,*]

[1] Scripps Center for Metabolomics and Department of Molecular and Computational Biology, The Scripps Research Institute, 10550 North Torrey Pines Road, La Jolla, CA 92037, United States

[2] Centre for Omic Sciences, EURECAT – Technology Centre of Catalonia & Rovira i Virgili University joint unit, Reus, Catalonia, Spain

[3] Discovery Chemistry, Genomics Institute of the Novartis Research Foundation, Metabolism and Pharmacokinetics, San Diego, California 92121, United States

[#]authors contributed equally

*Corresponding author

Gary Siuzdak, PhD

Scripps Center for Metabolomics

The Scripps Research Institute, La Jolla, CA 92037

Tel.: 858 784 9113

Email: siuzdak@scripps.edu

Table of Contents

Experimental Section

Materials. For the optimization of in-source fragmentation conditions, a mixture of 50 endogenous metabolites was prepared in water at 30 μM. These metabolites were selected to represent a broad range of physicochemical properties and metabolic pathways, such as amino acids, lipids, citric acid cycle, nucleotides, and coenzyme. For the investigation of sensitivity, a mixture of four metabolites in each ionization mode (tyrosine, inosine, uridine monophosphate (UMP), and oxidized glutathione in negative mode; phenylalanine, glutamine, histidine, and oxidized glutathione at positive mode) was prepared at 9 concentrations ranging 6 orders of magnitude: 1 nM, 10 nM, 100 nM, 1 μM, 10 μM, 50 μM, 100 μM, 500 μM, and 1 mM. The standards were purchased from Sigma-Aldrich (St. Louis, MO).

Metabolite extraction. Metabolites in the macrophage samples were extracted using the method described elsewhere with slight modifications.[1] In brief, cell samples were sonicated in ice for 15 mins after a shock-freezing in liquid nitrogen and subsequent thawing at room temperature. The operation was repeated for three times. Then the sample was incubated at – 20 °C overnight for protein precipitation, followed by centrifugation at 13, 000 rpm and 4 °C for 15 mins. The supernatant was dried in a vacuum concentrator and reconstituted with 50 μL acetonitrile:water (v:v; 1:1). After sonication (10 mins, in ice) and centrifugation (13, 000 rpm, 4 °C, 15 mins), the supernatant was transferred to a LC-MS glass vial for instrumental injection.

High-Resolution Mass Spectrometry Analysis. The metabolite mixture was analyzed with a liquid chromatography electrospray ionization quadrupole time-of-flight mass spectrometry (LC-ESI-QTOF-MS) (BRUKER impact II) in both positive and negative ESI modes. ZORBAX 300 SB-C18 column (0.5 × 150 mm, 5 μm, Agilent) and Luna® NH2 100 Å column (1 × 150 mm, 3 μm, Phenomenex) were used in the separation of metabolites in reverse phase (positive mode) and HILIC analysis (negative mode), respectively. For the reverse phase analysis, metabolites were separated by gradient elution at a flow rate of 20 μL/min starting at 5% (v/v) B, held for 5 min, increased to 95% B within 45 min, held for 5 min, and reverted to 5% B at 56th min, held for 5 min, with a total run time of 61 min. The mobile phases comprised water containing 0.1% formic acid (A) and acetonitrile containing 0.1% formic acid (B). For the HILIC analysis, metabolites were separated by gradient elution at a flow rate of 50 μL/min starting at 0% (v/v) A,

held for 1 min, increased to 100% A within 47 min, held for 5 min, and reverted to 0% A at 56th min, held for 5 min, with a total run time of 61 min. The mobile phases comprised water/acetonitrile (v/v; 95:5) containing 20 mM ammonium acetate and 40 mM ammonium hydroxide (A) and water/acetonitrile (v/v; 5:95) (B).

The original ESI source parameters were set as follows: dry temperature 180 °C, dry gas 7 L/min, nebulizer 20.3 psi, and capillary voltage 4500 V and – 4000 V for positive and negative modes, respectively. The transfer parameters were: funnel 1 RF 150 Vpp, funnel 2 RF 200 Vpp, isCID energy 0 eV, and hexapole RF 50 Vpp. The ion energy in the quadrupole was set to 4 eV and the collision energy applied in the collision cell was set at 7 eV. The instrument acquisition range was set at 50-1200 *m/z* and the MS acquisition rate was 2 spectra/s.

As discussed in the results section, transfer isCID energy was optimized to increase the in-source fragmentation while maintaining the intensity of precursor ions. After optimization, 30 eV and 40 eV transfer isCID energy were selected as the enhanced in-source fragmentation condition in positive and negative mode, respectively, with all other parameters fixed.

For the data dependent acquisition (DDA) of MS/MS spectra, both the MS and MS/MS acquisition rates were set at 2 spectra/s to acquire over the *m/z* range 50-1200. The collision energy was fixed at 20 eV for all the molecules, since a large number of small molecules generate specific fragments at 20 eV.

For the data independent acquisition (DIA) of MS/MS spectra, Broadband Collision Induced Dissociation (bbCID) mode was selected with low and high collision energy as 7 and 20 eV, respectively. isCID energy was set at 0 eV for both channel 1 (low collision energy) and 2 (high collision energy). The acquisition factors were set at 1 for both high and low collision energy. The low collision energy aims to provide full scan TOF MS spectra and the high collision energy is to generate the DIA MS/MS spectra for all the peaks without precursor isolation. The m/z range was set as 50-1200.

Single Quadrupole Mass Spectrometry Analysis. An Agilent InfinityLab Liquid Chromatography/Mass Selective Detector (LC-MSD) system was used in the single quadrupole MS based untargeted experiments. Poroshell 120 EC-C8 column (4.6 x 50 mm, 2.7 µm, Agilent) was used in the analysis of metabolite mixture in the positive mode; Acquity BEH Amide column (1 x 100 mm, 1.7 µm, 130 Å, Waters) was used in the negative mode. The gradient in

positive mode was as follows: starting at 5% (v/v) B, held for 2 min, increased to 95% B within 12 min, held for 2.5 min, and reverted to 5% B at 17th min, held for 3 min, with a total run time of 20 min; mobile phase A, water containing 0.1% formic acid (A); mobile phase B, acetonitrile containing 0.1% formic acid; mobile phase flow rate, 500 µL/min. The gradient in negative mode was as follows: starting at 1% (v/v) A, held for 1 min, increased to 35% A within 13 min, then increased to 60% A at 17th min, held for 1 min, and reverted to 1% A at 19th min, held for 6 min, with a total run time of 25 min; mobile phase A, water:acetonitrile (v:v; 95:5) containing 5 mM ammonium acetate and 5 mM ammonium hydroxide; mobile phase B, water:acetonitrile (v:v; 5:95); mobile phase flow rate, 100 µL/min.

The ESI source parameters were set as follows: in positive mode, drying gas flow 12 L/min, drying gas temperature 350 °C, nebulizer pressure 35 psig, and capillary voltage 4000 V; in negative mode, drying gas flow 8 L/min, drying gas temperature 325 °C, nebulizer pressure 30 psig, and capillary voltage 3500 V. Mass spectra was acquired over the m/z range of 50-1200 at two fragmentor voltages, 150 and 300 V, respectively.

Data Analysis. LC-MS and MS/MS datasets generated under different conditions were manually inspected with the Bruker Compass Data Analysis software (Version 4.4) to group the features (precursors and fragments) stemming from the same metabolite in high resolution MS based untargeted experiments. ChemStation software was used in the data analysis in single quadrupole MS based untargeted experiments. The targeted ion extraction window was ±0.01 m/z in high resolution MS data analysis and (-0.3, +0.7) da in single quadrupole MS data analysis.

eISA approach considers each molecule in the spectral library (e.g., METLIN) as an analysis target. By using this metabolite-centric approach, direct link between precursor ion and the fragments was established in the MS^1 data produced by eISA technique. The molecular identification procedure using eISA approach was shown as follows: (1) search the precursor ion m/z in the MS^1 chromatogram generated by eISA within a predefined window (e.g., ±0.01 m/z in high resolution MS data); (2) carefully select the peak of the precursor ion based on the retention time and acquire the compound spectra at the highest point of the peak; (3) record the in-source fragments of the precursor ion that matched to the reference spectral library based on the predefined mass accuracy criteria (e.g., 50 ppm in high resolution MS data); (4) evaluate the fragmentation pattern similarity between eISA technique and other techniques using two

matching scores, ratio score and match factor;[2] (5) assign putative molecular identification based on the fragmentation pattern similarity along with other orthogonal information (e.g., retention time). In this study, the MS/MS spectra generated at 20 eV in the METLIN library were used as reference spectra in molecular identification. Two indicators used in the molecular identification, ratio score and match factor, have been explained in details in our earlier study.[2] Briefly, ratio score was calculated as a fraction, with the denominator as the total number of fragments in the 20 eV MS/MS spectra in the METLIN library, unless stated otherwise. The numerator was the number of fragment ions in MS^1 (generated with eISA or DIA) or MS/MS (generated with DDA mode) that matched to the denominator. Match factor was calculated using the cosine dot product, a specific mathematical approach widely used in the determination of mass spectral similarity.[3] The match factor was calculated only for those metabolites with 3 or more fragments in their spectra. Match factor ranged from 0 to 100 (%), with 100 being the highest similarity match. Precursors were excluded from the computation of both ratio score and match factor. Further, only those fragments with over 5% relative intensity in the 20 eV MS/MS spectra in the METLIN database were used, unless all the fragments have relative intensities below 5% at 20 eV. The fragments outside the mass acquisition range (below 50 *m/z*) were not considered. Statistical analysis was conducted with GraphPad Prism 8.

In-Source Fragmentation Condition Optimization Results Section

This study aimed to find in-source fragmentation conditions in which more fragments can be generated without compromising the intensity of precursor ions (Fig. 1). Specifically, the aim was to generate mass spectral data including both the high abundance precursor ions and their corresponding in-source fragments for confident compound identification within a single run in full scan mode. The 20 eV MS/MS spectra in the METLIN library, produced in the collision cell with analytical standards, was used as a reference for the optimization process. We started with optimizing the electrospray ionization (ESI) source parameters such as capillary voltage and dry gas temperature to increase in-source fragmentation. Capillary voltage is known to control the desolvation/activation energy, which is directly related with the in-source fragmentation.[4,5] One purpose of dry gas within the source is to aid desolvation in electrospray source. Higher capillary voltage and dry gas temperature can facilitate the generation of in-source fragments.[4,5] In the BRUKER impact II, the suggested range of capillary voltage is 2000 to 5000 V in positive mode

and 1500 to 4000 V in negative mode, respectively; the suggested range of dry gas temperature is 180 to 240 °C, and the capillary voltage was set at 4500 V in positive mode and 4000 V in negative mode, respectively; the dry gas temperature was set up as 180 °C. Thus, we first increased the dry gas temperature to 240 °C to observe the impact on in-source fragmentation. As exemplified with four metabolites in Table S1, 1-palmitoyl-sn-glycero-3-phosphocholine and cytidine monophosphate in the positive mode and uridine and glucose-6-phosphate in the negative mode, increasing dry gas temperature does not significantly impact in-source fragmentation.

Next, we focused on the optimization of energy between ion funnel 1 and ion funnel 2, called the transfer isCID energy. The MS^1 spectra for the above mentioned four metabolites at two transfer isCID energies (20 and 40 eV) are shown in Table S1, where increasing transfer isCID energy from 0 (original setting) to 40 eV significantly improved the in-source fragmentation of selected molecules in both ionization modes.

To test the generality of this observation and find the appropriate transfer isCID energy for in-source fragmentation, we analyzed a mixture of 50 endogenous metabolites (30 μM) by varying transfer isCID (from 0 to 100 eV in 10 eV increments). These metabolites were all observed in negative mode and their MS/MS spectra at – 20 eV were all available in the METLIN library, however, in positive mode, only 33 metabolites were observed. Three factors were mainly considered in selecting the appropriate ISF condition: the number and relative intensity of fragments that matched to 20 eV MS/MS spectra in the METLIN database and the intensity of precursor ion.

To assess the in-source fragmentation performance, we first calculated the percentage of fragments of each metabolite generated at each condition versus the total number of fragments recorded in the 20 eV MS/MS spectra in the METLIN database. Only those fragments with a relative intensity above 5% were considered. As shown in Fig. S1a and S1b, the median fragment percentage observed in both positive and negative modes increased with the increase of isCID energy. A similar trend was also observed for match factor (Fig. S1c and S1d), which was calculated for those metabolites with at least 3 fragments in the 20 eV MS/MS spectra in the METLIN database to assess the relative intensity similarity. The relationship between the median value of 1^{st} top fragment intensity of each metabolite versus the isCID energy exhibited a reversed U-shaped curve (Fig. S1e and S1f), especially in the positive mode. This indicates that

there are optimal and consistent settings across a wide variety of molecules for consistently creating fragments that facilitate identification. We further evaluated these setting with respect to intensity loss of precursor ion and as expected, the intensity of the precursor ion decreases with an increase of isCID energy (Fig. S1g and S1h).

Based on the results observed, we selected 40 eV and 30 eV isCID energy as the eISA condition in negative and positive mode, respectively, with all other parameters fixed. Compared with the original in-source condition (isCID energy is 0 eV), the MS^1 spectra acquired at 40 eV isCID energy in the negative mode shows better fragmentation pattern: 37% increase in median percentage of fragments (up to 100% in over half cases), 15% increase in median match factor, and 3.2 times increase in the median intensity of 1st top fragment ion (Fig. S1a,c,e). Further, as compared with higher isCID energies, a more constant precursor ion intensity (a median loss of only 9%) is observed when isCID energy is 40 eV (Fig. S1g). In the positive mode, MS^1 spectra at 30 eV isCID energy has a close median match factor and major fragment ion intensity with the original in-source fragmentation condition, but it has higher median percentage of fragments, 96%, which is close to what was observed at higher isCID energies (100% at 40 eV and higher energies) (Fig. S1b,d,f). More importantly, the median loss of precursor ion intensity at this condition is only 7% lower, however, this number is 47% at 40 eV isCID energy, although significantly improved fragmentation data was achieved (Fig. S1h). These results indicate that it is possible to generate in-source fragments comparable with higher energy MS/MS spectra by enhancing ISF condition in the ESI source, while maintaining the intensity of precursor ion.

REFERENCES

(1) Warth, B.; Raffeiner, P.; Granados, A.; Huan, T.; Fang, M.; Forsberg, E. M.; Benton, H. P.; Goetz, L.; Johnson, C. H.; Siuzdak, G. Metabolomics reveals that dietary xenoestrogens alter cellular metabolism induced by palbociclib/letrozole combination cancer therapy. *Cell Chem Biol* **2018**, *25*, 291-300 e293.

(2) Domingo-Almenara, X.; Montenegro-Burke, J. R.; Guijas, C.; Majumder, E. L.; Benton, H. P.; Siuzdak, G. Autonomous METLIN-guided in-source fragment annotation for untargeted metabolomics. *Anal Chem* **2019**, *91*, 3246-3253.

(3) Kim, S.; Zhang, X. Comparative analysis of mass spectral similarity measures on peak alignment for comprehensive two-dimensional gas chromatography mass spectrometry. *Comput Math Methods Med* **2013**, *2013*, 509761.

(4) Purvine, S.; Eppel, J. T.; Yi, E. C.; Goodlett, D. R. Shortgun collision-induced dissociation of peptides using a time of flight mass analyzer. *Proteomics* **2003**, *3*, 847-850.

(5) Ramos, A. A.; Yang, H.; Rosen, L. E.; Yao, X. Tandem parallel fragmentation of peptides for mass spectrometry. *Anal Chem* **2006**, *78*, 6391-6397

Table S1. Absolute (relative) intensities comparison (including both precursor ions and fragments) for metabolites across different in-source fragmentation conditions and METLIN library at both positive mode (1-palmitoyl-sn-glycero-3-phosphocholine and cytidine monophosphate) and negative mode (glucose-6-phosphate and uridine)

analyte	m/z	absolute (relative) intensity					relative intensity
		dry gas temperature (°C)		isCID energy (eV)			METLIN (20 eV)
		180	240	0	20	40	
1-palmitoyl-sn-glycero-3-phosphocholine (ESI(+))							
precursor ion	496.34	9896886	9789667	9896886	9289506	8081574	
fragment 1	104.105	0	0	0	0	20488 (100)	54
fragment 2	184.069	0	0	0	0	11562 (56)	100
fragment 3	478.319	14480	15260	14480	11520	13658 (67)	10
cytidine monophosphate (ESI(+))							
precursor ion	324.053	133396	145672	133396	139096	86498	
fragment 1	97.029	5142 (0.3)	5230 (0.3)	5142 (0.3)	7032 (0.3)	15258 (0.4)	5
fragment 2	112.048	1814604 (100)	1867800 (100)	1814604 (100)	2120736 (100)	4135146 (100)	100
glucose-6-phosphate (ESI(-))							
precursor ion	259.022	454652	468930	454652	475116	329692	
fragment 1	78.959	1672 (2)	1749 (2)	1672 (2)	2610 (3)	14110 (30)	38
fragment 2	96.9693	57424 (60)	56390 (59)	57424 (60)	49550 (52)	47024 (100)	100
fragment 3	138.978	95464 (100)	96480 (100)	95464 (100)	95368 (100)	24776 (53)	8
uridine (ESI(-))							
precursor ion	243.062	3674204	3756890	3674204	3928470	3615684	
fragment 1	66.0347	0		0	0	7134 (3)	15
fragment 2	82.0301	0		0	0	18696 (8)	37
fragment 3	110.025	41574 (100)	42750 (100)	41574 (100)	40960 (100)	242978 (100)	100
fragment 4	122.024	0		0	0	14958 (6)	11
fragment 5	152.034	16796 (40)	17840 (42)	16796 (40)	21004 (51)	75444 (31)	8
fragment 6	153.03	13222 (32)	14630 (34)	13222 (32)	18756 (46)	62994 (26)	6

Table S2. Absolute (relative) intensities comparison of both precursor ions and fragments of tyrosine at different levels acquired with QTOF DDA (20 eV) and eISA techniques

tyrosine ESI(-)		absolute (relative) intensity										relative intensity
		QTOF DDA					eISA					METLIN (20 eV)
		1nm	10nm	100nm	1μm	10μm	1nm	10nm	100nm	1μm	10μm	
Precursor ion	180.06	292	272	458	302	1250	1228	984	1542	3714	13146	-
fragment 1	72.007	162 (100)	0	160 (80)	0	0	0	0	0	0	0	42
fragment 2	93.033	0	0	0	236 (54)	0	0	172 (73)	0	0	254 (21)	27
fragment 3	119.05	0	166 (100)	200 (100)	438 (100)	2870 (100)	438 (100)	218 (92)	190 (93)	410 (55)	1234 (100)	100
fragment 4	163.04	146 (90)	0	170 (85)	246 (56)	694 (24)	394 (90)	236 (100)	204 (100)	748 (100)	660 (54)	25

Table S3. Instrumental sensitivity comparison of the quadrupole time of flight mass spectrometry (QTOF) at three different modes with select metabolites.

analyte	mode	target ion	RT[a] (min)	LOD[b] (nM)		
				eISA	QTOF DIA	QTOF DDA
tyrosine	ESI(-)	180.0666	17.3	1	1	100
inosine	ESI(-)	267.0735	16.6	1	1	1
UMP	ESI(-)	323.0286	31.8	1	1	1
oxidized glutathione	ESI(-)	611.1447	32.4	1	1	1
glutamine	ESI(+)	147.0764	6.9	1000	1000	10000
histidine	ESI(+)	156.0766	6.7	1	1	100
phenylalanine	ESI(+)	166.0863	7.7	1	1	100
oxidized glutathione	ESI(+)	613.1592	7.1	10	100	100

[a]RT: retention time; [b]LOD: limit of detection.

Table S4. Fragmentation pattern comparison between mass spectra acquired in the eISA mode and QTOF DIA mode (20 eV)

no.	ESI (-)			ESI (+)		
	name	score[a]	M.F.[b]	name	score	M.F.
1	aspartate	4/4	96			
2	malate	4/4	40			
3	adenine	2/4	100	adenine	2/3	100
4	hypoxanthine	2/3	100	hypoxanthine	2/5	98
5	sulfoacetic acid	2/2				
6	glutamine	8/9	93	glutamine	3/3	61
7	glutamate	2/2		glutamate	3/3	84
8	methionine	1/1		methionine	6/7	55
9	xanthine	2/2*	100	xanthine	1/4	100
10	aminoadipic acid	5/5*	16	aminoadipic acid	4/5	81
11	phenylalanine	4/5	89	phenylalanine	2/2	
12	phosphoenol pyruvate	1/1				
13	uric acid	4/4	99			
14	glyceraldehyde-3P	2/2				
15	arginine	1/1		arginine	4/4	54
16	tyrosine	3/4	92	tyrosine	8/9	80
17	acetyl-glutamic acid	5/6	33	acetyl-glutamic acid	4/4	91
18	citric acid	5/5	97			
19	tryptophan	4/4	96	tryptophan	7/7	62
20	myristic acid	0/0				
21	ribose-5-phosphate	3/3	55			
22	cytidine	5/5	100	cytidine	1/1	
23	uridine	6/6	100	uridine	1/3	100
24	palmitic acid	0/0		palmitic acid	12/12	78
25	glucose-6-phosphate	3/3	94	glucose-6-phosphate	5/6	97
26	fructose-6-phosphate	3/3	94	fructose-6-phosphate	2/2	
27	adenosine	1/1		adenosine	1/1	
28	inosine	1/1		inosine	1/1	
29	saccharopine	7/13*	98	saccharopine	2/4	68
30	linoleic acid	0/0				
31	oleic acid	0/0		oleic acid	23/25	83
32	guanosine	3/3	6	guanosine	1/1	
33	EPA	2/7	25			
34	CMP	3/3	74	CMP	2/2	
35	UMP	6/6	80	UMP	2/2	
36	fructose-1,6-bisphosphate	5/5	94			
37	AMP	3/3	74	AMP	1/1	
38	IMP	3/5	84	IMP	1/2	
39	GMP	3/3	58	GMP	1/2	
40	UDP	4/9	16			
41	ADP	5/7	30	ADP	2/3	100
42	GDP	4/6	23	GDP	1/1	
43	PG(16:0/0:0)	1/3	98	PG(16:0/0:0)	2/3	100
44	lysoPC(16:0)	1/3	100	lysoPC(16:0)	1/3	25
45	GTP	9/9*	46			
46	UDP-galactose	3/6	14			
47	UDP-N-acetyl-glucosamine	5/8	80			
48	oxidized glutathione	10/10	76	oxidized glutathione	5/9	76
49	dioleoylphosphatidic acid	2/3*	73			
50	acetyl-CoA	4/4	78	acetyl-CoA	4/6	71

[a]score: ratio score; [b]M.F.: match factor; *: the number of fragments found in the QTOF DIA mode is less than that recorded in the 20 eV mass spectra in the METLIN database; the calculation of both score and M.F. was based on the 20 eV MS/MS spectra produced in the QTOF DIA mode.

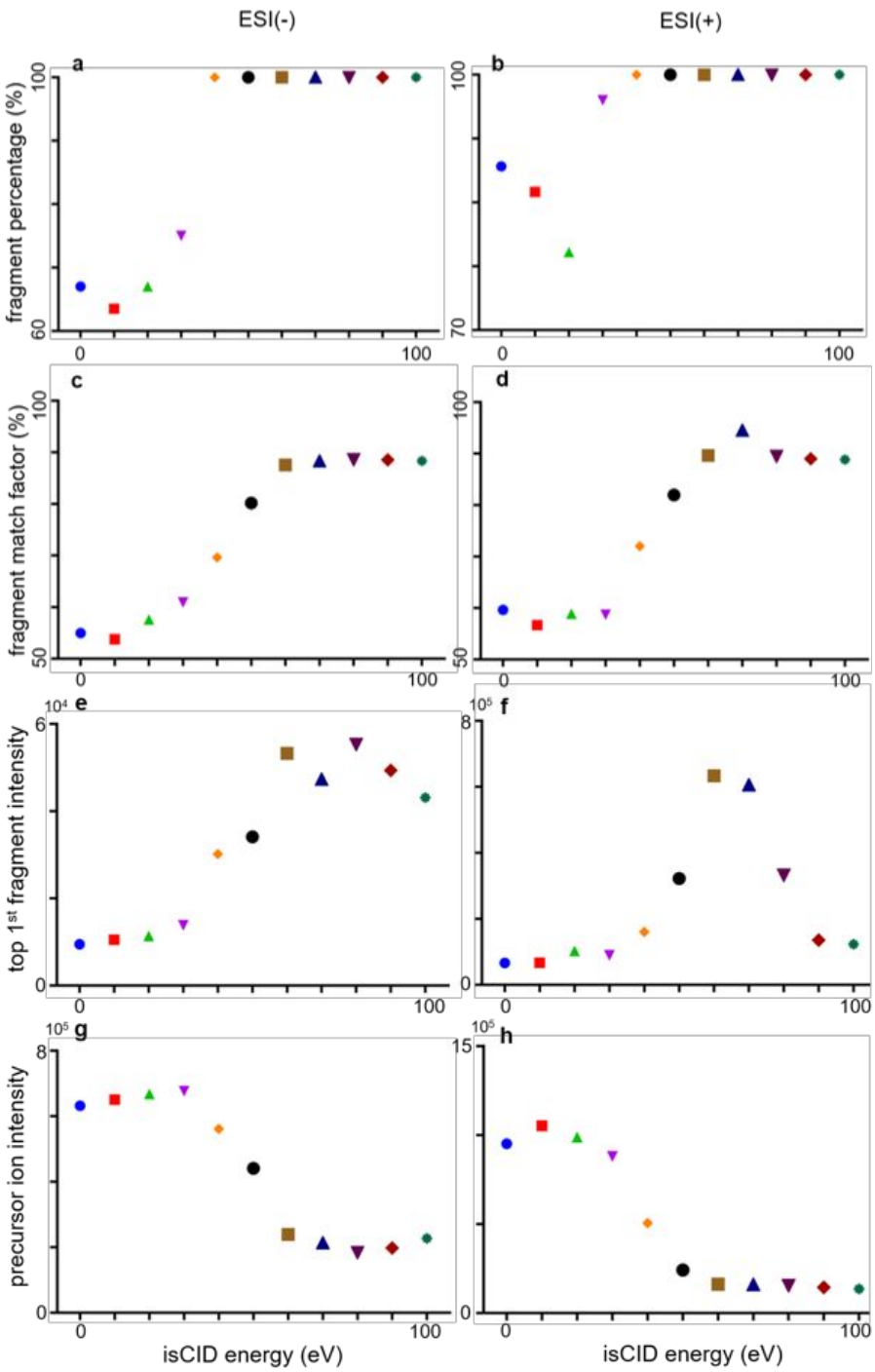

Figure S1. Panels (a) and (b) plot the relationship between median fragment percentage and isCID energy. Panels (c) and (d) plot the relationship between median fragment match factor versus isCID energy. Panels (e) and (f) plot the relationship between median intensity of the major (1st top) fragment ion versus isCID energy. Panels (g) and (h) plot the relationship between median intensity of the precursor ion versus isCID energy. Panels (a), (c), (e), and (g) were observed at negative mode (ESI(-)) and others were observed at positive mode (ESI(+)). Both fragment percentage and match factor were calculated versus the +/- 20 eV MS/MS spectra in the METLIN database.

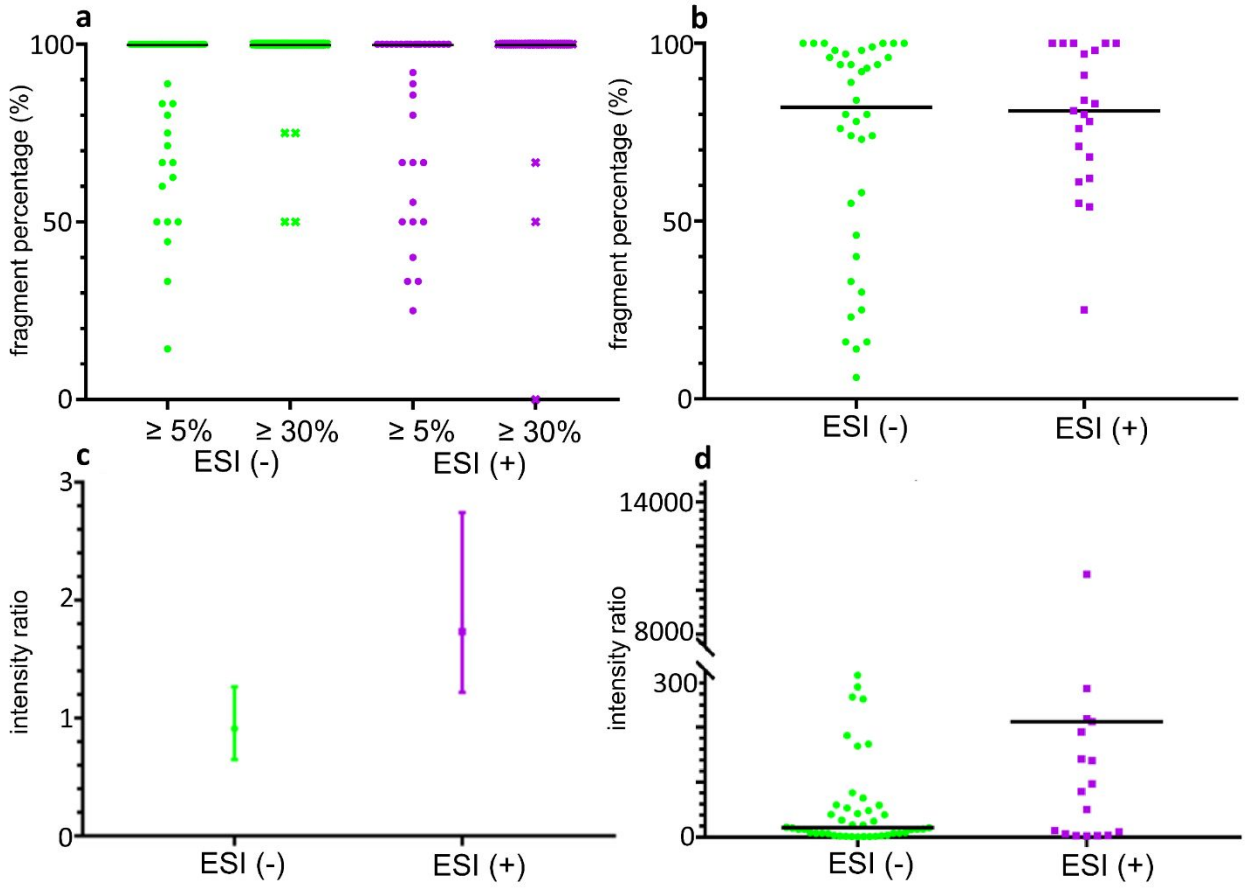

Figure S2. The percentage of fragment produced at eISA mode versus QTOF DDA mode increases with the increase of relative intensity of fragments (from ≥ 5% to ≥ 30%) considered at both ionization modes with black line representing media (a). Panel (b) shows the vertical scatter plot with median fragment match factor (eISA vs. QTOF DDA) across different polarity modes. Panel (c) shows the absolute intensity ratio (median plus 95% CI) of fragments generated by eISA versus those generated with QTOF DDA technique. Panel (d) shows the absolute intensity ratio (median plus 95% CI) of precursor ions generated by eISA versus those generated with QTOF DDA technique. MS/MS spectra in the QTOF DDA mode was generated at 20 eV.

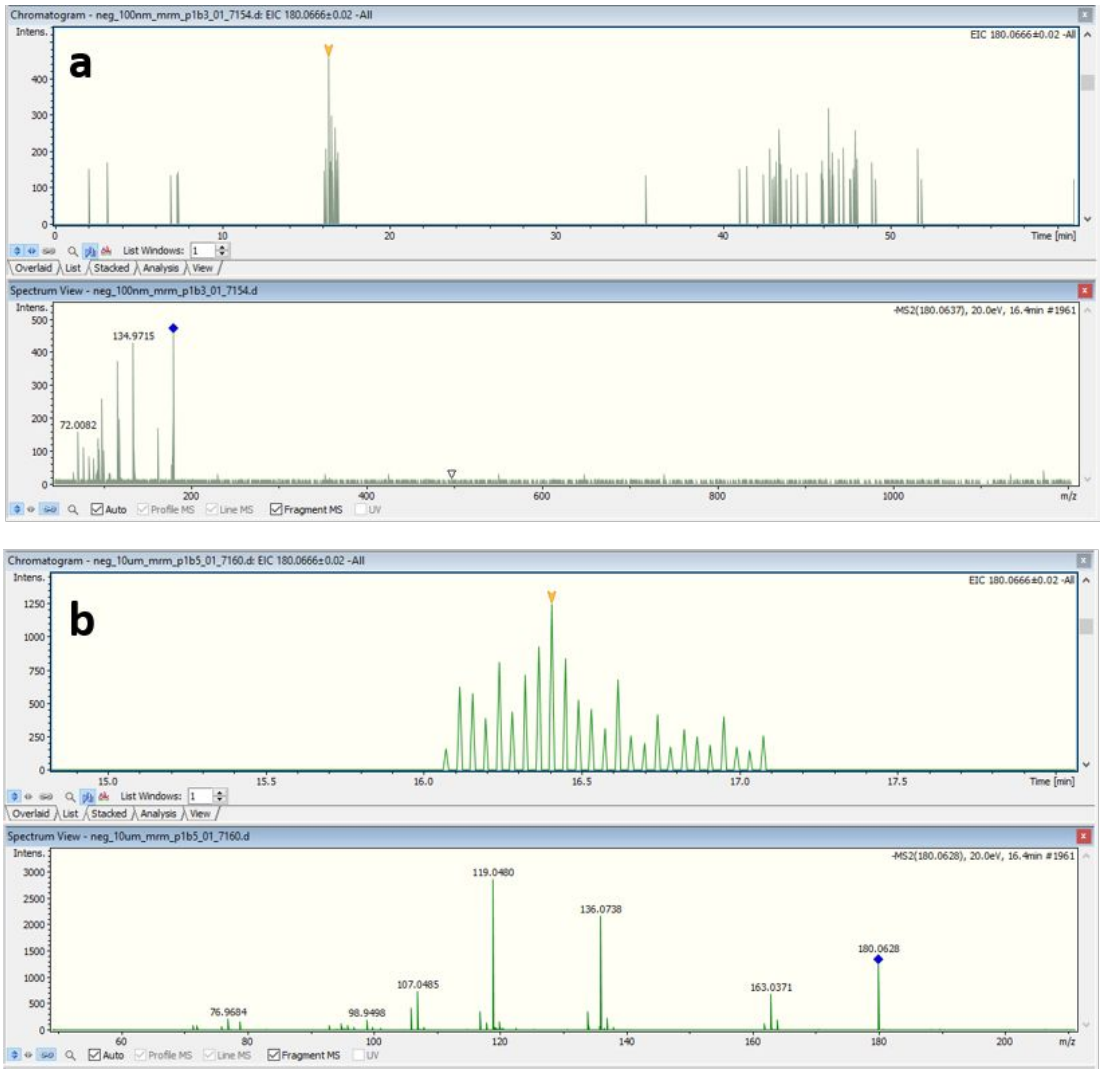

Figure S3. MS/MS spectra of tyrosine acquired at 100 nM (a) and 10 μM (b) using QTOF DDA mode (ESI(-)).